Available online at www.sciencedirect.com

Polymer 47 (2006) 1612–1619

polymer

www.elsevier.com/locate/polymer

Photopolymerization and structure formation of methacrylic acid based hydrogels in water/ethanol mixture

Hongyan He, Ling Li, L. James Lee *

Department of Chemical and Biomolecular Engineering, The Ohio State University, Columbus, OH 43210, USA

Received 30 September 2005; received in revised form 27 December 2005; accepted 4 January 2006

Abstract

Hydrogels are a desired material for biomedical and pharmaceutical applications. To better control the synthesized hydrogels for various applications, it is necessary to have a thorough understanding of hydrogel structure and reaction mechanism. In this study, pH-sensitive hydrogel networks consisting of methacrylic acid (MAA) crosslinked with tri(ethylene glycol) dimethacrylate (TEGDMA) were synthesized by free-radical photopolymerization in the water/ethanol mixture. Reaction rate was measured using Photo-differential scanning calorimetry (PhotoDSC) with a modified sample pan designed for handling volatile reagents. A photo-rheometer and a dynamic light scattering (DLS) goniometer were used to follow the changes in viscosity and molecule size of the resin system during photopolymerization. It was found that the rate of polymerization increased and more compact and less swelling gels would form with a higher water fraction in 50 wt% solvent/reactant mixture. This is because the weaker interactions between the MAA and the solvent give a higher opportunity for propagation and a higher reaction rate. And the hydrophobic TEGDMA and initiator tend to form aggregates in the higher water solution, contributing to the inhomogeneous microgel formation. This mechanism is conformed by viscosity measurement, DLS analysis, scanning electron microscopy (SEM) observation, and kinetics analysis.

Keywords: Photopolymerization of hydrogels; Water/ethanol composition; Viscosity change

1. Introduction

Hydrogels are a desired material for biomedical and pharmaceutical applications due to their unique swelling properties and structures. The highly hydrated structure and good biocompatibility make them suitable for contact lenses, biosensors, artificial organs, and drug delivery devices [1,2]. In drug delivery, functional hydrogels may release drugs in an aqueous median at regulated rate by controlling the synthesis conditions such as the method of polymerization, the crosslinking ratio, and the solvent composition.

Hydrogels are often synthesized by UV photopolymerization [3,4] or redox polymerization [5]. Photopolymerization is favored because hydrogels can be synthesized at temperatures and pH conditions near physiological conditions and even in the presence of biologically active materials. Furthermore, photopolymerization can be easily controlled by adjusting the dosage and intensity of UV light, and the curing temperature [6]. Photo-differential scanning calorimetry (PhotoDSC) is the most widely used technique to characterize the photopolymerization kinetics. A great deal of research has been carried out using this approach for photocurable materials. However, the application of this technique for highly volatile reagents is limited since uncovered sample pans lead to significant sample loss during measurement. Some researchers applied unsealed polyethylene (PE) films over the sample pan to reduce the sample loss [4], while others used the sample weight after the reaction to correct for the measurement error resulting from reagent evaporation [7]. The results from such treatments are doubtful because sample loss during the reaction is a time-dependent process. When preparing the carriers for drug delivery, solvents like water and ethanol are often used in the synthesis to control the hydrogel structure. Evaporation of highly volatile solvents like ethanol makes it impossible to study the reaction kinetics using the existing approaches. We have recently developed a modified DSC sample pan [8]. Sample loss during reaction is minimized, and loaded samples are much more uniform over the sample surface. This new method is applied in this study.

To better control the synthesized hydrogels for various applications, it is essential to understand how the polymerization conditions, chemical structure of reactants and their composition, and solvent type and concentration affect the

---

* Corresponding author. Tel.: +1 614 292 2408; fax: +1 614 292 3769.
E-mail address: leelj@chbmeng.ohio-state.edu (L.J. Lee).

0032-3861/$ - see front matter © 2006 Elsevier Ltd. All rights reserved.
doi:10.1016/j.polymer.2006.01.014

reaction and the resulting properties of hydrogels. A number of studies have reported that varying curing conditions may achieve different gel structures and swelling properties [9–14], and the compatibility between the solvent and the resin may affect inter-molecular and primary cyclization of multi-vinyl monomers during the polymerization, and, consequently, the hydrogel properties [12–14]. However, there lacks a thorough understanding on the interactions of reaction kinetics, rheological changes, hydrogel structures, and solvent–resin compatibility. In this study, PMAA gels synthesized in a water/ethanol mixture were investigated by using a series of analytical tools including PhotoDSC, photo-rheometry, dynamic light scattering goniometry, and scanning electron microscopy of freeze–dried hydrogels.

2. Experimental

2.1. Materials and sample preparation

The monomer, MAA (Sigma-Aldrich) and the crosslinking agent, TEGDMA (Sigma-Aldrich) were used to prepare pH-sensitive hydrogels. For all reactions, the crosslinking agent was presented at a level of 1.0 mol% based on the total mole of monomers. A photoinitiator, 2,2-dimethoxy-2-phenylacetophenone (Irgacure 651, Ciba Specificity Chemicals), was used at 1.0 wt% of the monomer mixture. The free-radical photopolymerization was carried out in a mixed solvent of distilled water and ethanol with varying ratios. The ratio of monomer to solvent was kept at 50:50 (w/w). All reagents, unless specified, were of analytical grade and were used without further purification.

To prepare hydrogel films for the swelling test and structure analysis, 5.0 g of MAA were mixed with a proper amount of TEGDMA and initiator. An equal weight of solvent mixture was then added. The solution was transferred to a glove box where it was kept under a nitrogen atmosphere. Nitrogen was bubbled through the solution for 20 min. Then the mixture was pipetted between two glass slides separated by a Teflon spacer. The thickness of the spacers was 0.3 mm. The setup was then placed under a UV light for photopolymerization at 2.0 mW/cm^2. The cured hydrogels were then rinsed in double deionized water for 5 days to remove unreacted monomer, initiator and sol fraction. Subsequently, the monomer-free films were cut into samples with a 5.0 mm diameter for swelling test.

2.2. PhotoDSC measurements

The reaction kinetics and heat of reaction of PMAA gels were measured using a PhotoDSC (TA 2920, TA Instruments). A UV light source (Novacure, 100 W Hg short-arc lamp, EXFO, Mississaugua, Ont., Canada) was used to cure the samples. In order to prevent the weight loss of volatile MAA and ethanol, the DSC pans were physically and chemically modified by using the technique described elsewhere [8]. We compared the performance of modified sample pans vs. the ones covered with a layer of PE film. A micropipette was used for PhotoDSC sampling (5–7 μl), which controlled the sample weight for each test. All measurements were carried out at 30 °C and the light intensity was kept at 2.0 mW/cm^2. Each run was conducted by purging the sample with nitrogen gas until reaching equilibrium (around 2 min), and then UV irradiation was applied to induce the free-radical polymerization.

2.3. Rheological measurements

A photo stress rheometer MCR 300 (Physica, Anton Paar) was used to follow the viscosity change during the isothermal photopolymerization. A UV cell, including a top steel plate with a diameter of 50 mm and a bottom plate made of quartz glass, was utilized in this test. The UV light source (Acticure 4000, EXFO, Canada) was illuminated from the bottom. The light intensity on the sample surface was kept at 2.0 mW/cm^2. The gap between the two plates was set at 1.0 mm and the shear rate used was 0.1 s^{-1}. The gel point was assumed when the relative viscosity, i.e. viscosity of the reactive resin vs. its initial viscosity, reached 10^4.

2.4. Dynamic light scattering analysis

Dynamic light scattering (DLS) measurements at 30 °C were carried out to determine the molecule size and size distribution before gelation during photopolymerization by using a BI-DNDC differential refractometer (Brookhaven Instruments) with a 10 mW He–Ne laser beam at a wavelength of 633 nm. A scattering angle was held constant at 90° in the measurement. Before the DLS analysis, the partially reacted sample (around 0.3 ml) was dispersed in 3 ml of ethanol, and the diluted solution was then filtrated through a filtration unit with 0.45-μm pore size (Whatman Puradisc 25TF). Count rates between 10 and 200 kilocounts/s were used to obtain meaningful results by changing the sample concentration and adjusting the laser power. Autocorrelation of the intensity was carried out by the method of cumulate analysis to obtain an average diameter of the molecules and the polydispersity. The molecule size distribution was obtained from the correction function by CONTIN analysis using the standard software BI-DNDCW.

2.5. Swelling tests

The swelling tests were performed at various pH values ranging from 2.6 to 7.4 to characterize the swelling behavior for synthesized pH-sensitive hydrogels. The buffer solutions with different pH values were prepared by mixing the citric acid with appropriate amounts of sodium phosphate solution. Sodium chloride was used to adjust the ionic strength of all solutions to $I=0.1$ M, which is the near-physiological condition. The dried hydrogel samples were weighed and placed in the buffer solution at room temperature (25 °C). The samples were taken out of the solution at pre-selected time intervals. After the extra water on the surface was removed by laboratory tissue, the weight of the wet hydrogels was measured. The weight-swelling ratio was calculated by the weight of the swollen sample to the weight of the dried sample. The samples were blotted and weighed until the weight change is less than 0.1 mg over a 24 h period.

2.6. Scanning electron microscopy

To visually examine the surface and interior morphology of hydrogels in the swollen state, a Hitachi Model S-4300 SEM was used to analyze the pore structure. The samples cured under UV radiation were first swollen to reach equilibrium in buffer solutions for 24 h, and then quickly frozen below its freezing point using liquid nitrogen. The sample containers were transferred to a freeze–dryer (Labconco 75150, Labconco Inc. Kansas City, MI) and freeze–dried for 48 h until all solvent was sublimed. The freeze–dried samples were loaded on the surface of an aluminum SEM specimen holder and sputter coated with gold for 40 s (Pelco Model 3 Sputter Coater) before observation. A working distance about 8–10 mm, an accelerating voltage of 10 kV, and a chamber pressure of 10^{-8} Torr were found to be suitable for obtaining high-resolution images of hydrogel samples. The magnification in this study varied from 2000× to 20,000× depending on the network structure.

3. Results and discussion

An important feature of this curing system was the formation of heterogeneous structure in different solvent compositions, which influenced not only the reaction kinetics and rheological changes of the resin, but also the swelling behavior and network structure of the formed gels.

3.1. Kinetics of MAA/TEGDMA photopolymerization

To minimize the sample weight loss during DSC measurements, the sample pan was physically and chemically modified. The advantage of such treatment was demonstrated via the photopolymerization of the MAA/TEGDMA system. The measured heat flow by using both modified and un-modified pans is shown in Fig. 1. With a modified sample pan, an equilibrium state was reached in about 1–2 min, and the measurement started at a level close to the 'zero' heat flux. While, with a regular sample pan covered with a layer of PE film, there was a continuous endotherm due to the evaporation of monomers and solvents, leading to a negative starting point for heat flux. Additionally, a longer time was needed to reach equilibrium, which would inevitably cause more weight loss. For systems containing highly volatile MAA and ethanol, a strong competition occurred between sample evaporation and chemical reaction. Consequently, a complete change in the reaction rate profile was observed with the use of an un-modified DSC pan. The sample weights before and after the test showed that there was less than 5% weight loss using a modifies pan, compared to about 40% loss using an un-modifies pan (the data represents the mean of six samples). It is clear that the modified pans have to be used in the DSC kinetic analysis of volatile monomers and solvents.

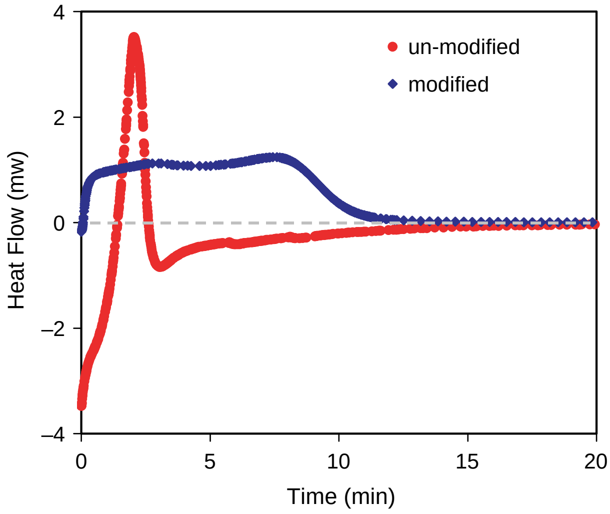

Fig. 1. Comparison of PhotoDSC measurements by using a modified and an unmodified pan at UV intensity of 2.0 mW/cm^2 in the MAA/TEGDMA system (1.0 mol%TEGDMA, 50 wt% solvent mixture of the 1:1 water/ethanol ratio).

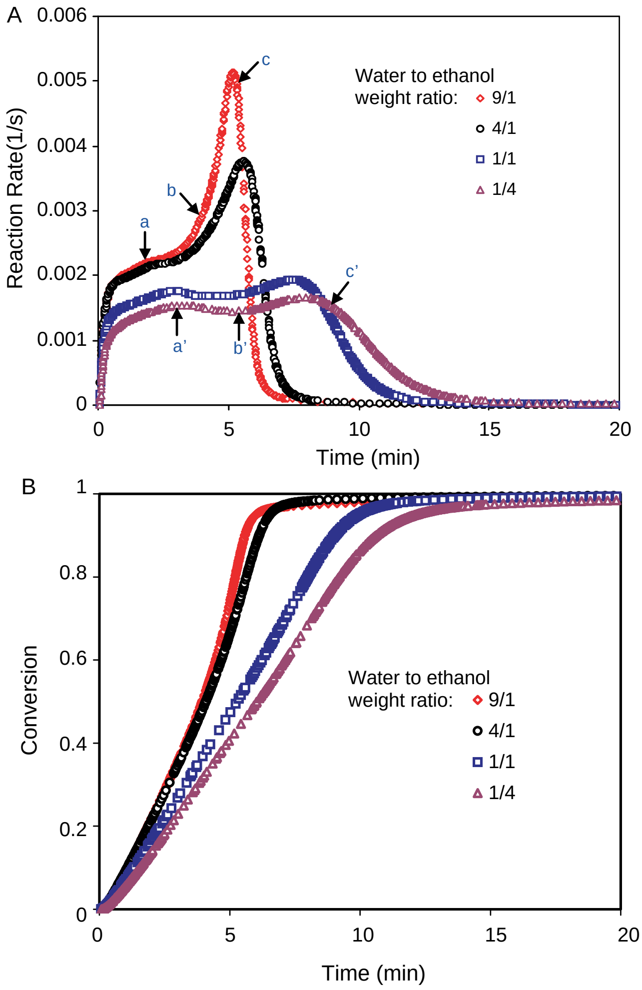

Fig. 2. (A) Reaction rate and (B) conversion versus reaction time for the isothermal photopolymerization of MAA/TEGDMA (1.0 mol% TEGDMA, 50 wt% solvent) with different solvent compositions at 30 °C and UV intensity of 2.0 mW/cm^2.

Using the modified pans, the effect of solvent composition on the reaction kinetics of MAA/TEGDMA was investigated. Fig. 2(A) shows the reaction rate versus reaction time for the isothermal photopolymerization of MAA/TEGDMA (1.0 mol% TEGDMA, 50 wt% solvent) with different solvent compositions at 30 °C and a UV intensity of 2.0 mW/cm^2. As can be seen, the solvent composition had a great influence on the reaction kinetics of the photocurable MAA/TEGDMA system. With an increase of the ethanol content in the solvent mixture, the polymerization rate decreased correspondingly, and multiple exothermic peaks were observed on the reaction rate profiles for all cases. A peak occurred at the very early stage of polymerization, followed with a stronger second peak. A higher ethanol content delayed and broadened the first peak and substantially reduced the second peak. It is also noted from the conversion profiles shown in Fig. 2(B) that the higher ethanol content delayed the time to achieve a high conversion.

The multiple peaks observed in the free radical crosslinking polymerization have been reported for several mono- and divinyl monomers [7,8,15–18]. Horie and coworkers [16] postulated that the double maxima in the reaction rate of MMA/EGDM systems were caused by microgel formation. They attributed the first peak to the Trommsdorff effect in the bulk material while the resin mixture was still homogeneous, and the second one to the Trommsdorff rate acceleration in the microgels. As the polymerization proceeded further, the system viscosity limited propagation and the autodeceleration in the reaction rate occurred, as monomer could not diffuse to the relatively immobile radicals. Such hypothesis has also been used to interpret the occurrence of multiple reaction peaks in the acrylic acid (and *N*-vinylpyrrolidone) copolymerization with TEGDMA [7], in the photopolymerization of HEMA/glycerin [16], in the photopolymerization of a series of oligo (methylene) oxide and oligo (ethylene oxide) dimethacrylates [17], and in the reaction between multifunctional methacrylate and acrylate monomers [18]. Although our kinetics results show a similar trend, the viscosity and molecule size analysis presented in the next section, however, show a different mechanism.

3.2. Viscosity measurement and molecule size analysis

In order to evaluate the effect of solvent composition on the polymeric structure formation, rheological and DLS measurements were carried out to follow the viscosity change and the growth of molecule size during photopolymerization. Fig. 3(A) displays both the relative viscosity and reaction rate as a function of double bond conversion for PMAA gels with different solvent compositions. Approaching the gel point, there was the steep increase of relative viscosity (10^4). For the gels with the water/ethanol ratio of 1:4, the macrogelation occurred at 9 min or around a conversion of 78%. With an increase of water content, the curves of relative viscosity shifted to a higher conversion. Fig. 3(B) presents the corresponding gel time and gel conversion versus water content based on the weight of solvent mixture. The gelation time was linearly decreased and the gel conversion was increased with the increasing water content. For the system with the highest water content 1, it only took around 5.5 min to reach the gel point. However, its gel conversion could reach 88%.

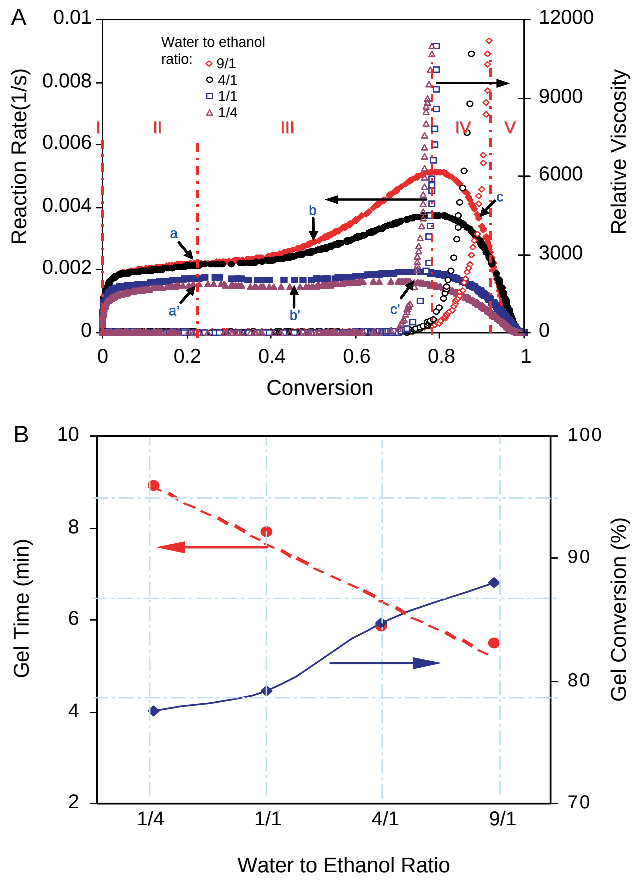

Fig. 3. (A) Reaction rate and viscosity rise as a function of conversion of MAA/TEGDMA (1.0 mol% TEGDMA, 50 wt% solvent) with different solvent compositions cured at UV intensity of 2.0 mW/cm^2. (B) Gel time and gel conversion versus water/ethanol ratio in the solvent mixture.

Fig. 4(A) and (B) summarizes the size distribution of polymers formed during the photopolymerization of MAA/TEGDMA in ethanol. For MAA/TEGDMA with the 1:4 solvent ratio, the double bond conversion was around 78% at the gel point. The macromolecules formed at a conversion of 23% (point ‘a’, the first maxima of reaction rate in Figs. 2(A) and 3(A)) exhibited a narrow unimodal size distribution, ranging from 5 to 80 nm. The intensity reached the maximum value at 17.5 nm. With the reaction progressed to a conversion of 45% (point ‘b’, onset of the second autoacceleration in Figs. 2(A) and 3(A), the peak was shifted to 64 nm. In addition, a bimodal size distribution occurred, which contains a very narrow peak (13–32 nm) with the same maximum value at 17.5 nm and a broader and larger size distribution (40–164 nm). A further increase in the conversion to 76% (point *c*, before macrogelation) showed very large clusters with the size distribution from 3 to 223 nm, while the intensity ratio of smaller molecules decreased significantly. Apparently, most small molecules had converted into larger clusters.

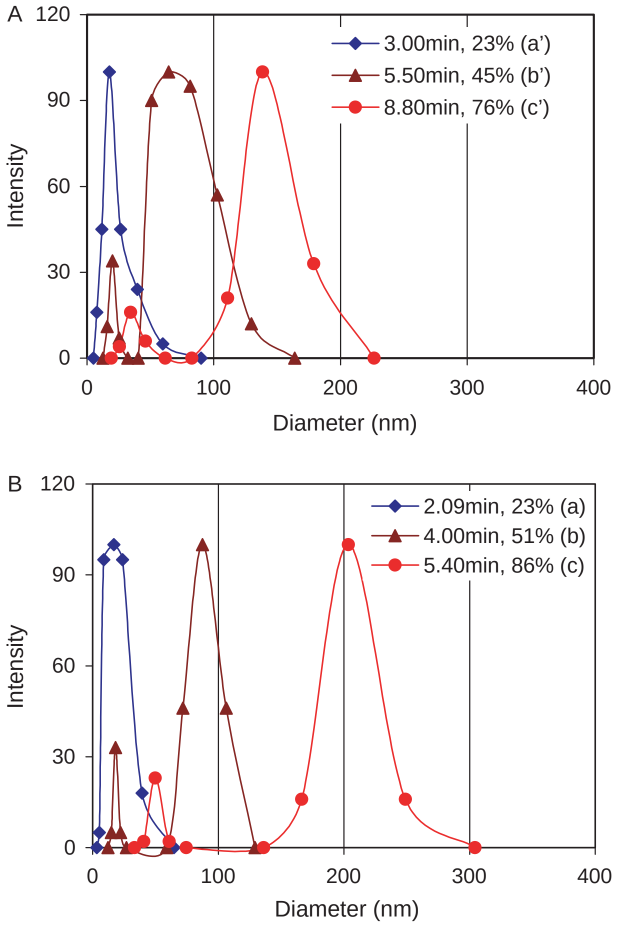

Fig. 4. The size distribution of MAA/TEGDMA resin (1.0% TEGDMA, 50 wt% solvent) with different solvent ratios of water/ethanol: (A) 1:4 and (B) 9:1 cured at light intensity of 2.0 mW/cm^2.

Compared with the system with the 1:4 solvent ratio, the size distribution curves for the system with the 9:1 solvent ratio exhibited a similar shape and trend. Increasing the water content in the solvent mixture shifted the polymer size distribution to a larger size. For example, the formed polymer showed a unimodal size distribution at the same conversion of 23%, point a', and a bimodal size distribution around the onset of the second autoacceleration, point b', except that the molecule clusters were large. At a conversion of 86%, point c' which was close to the gel conversion, the peak for larger molecules moved to 204 nm and the width of the distribution spread from 136 to 304 nm. Obviously, the resin system with a higher water/ethanol ratio formed larger polymer clusters under the same UV radiation when the reaction approached macrogelation.

3.3. Mechanism for gelation

It is well known that free-radical polymerization of multifunctional monomers forms heterogeneous polymer networks, leading to microgel formation [8,16–21]. Such entities are a result of strong intramolecular crosslinking of the growing macroradicals. Eventually, intermolecular reactions among microgels form the network structure. The relative rates of intra- and intermolecular reactions depend on the initial monomer composition, as well as other reaction conditions. The solvent composition is a major factor influencing the gelation kinetics. According to the experimental results shown in the previous section, the photopolymerization of MAA/TEGDMA system can be described in five stages: initiation, microgel formation, cluster formation, macro-gelation, and post-gelation. The schematic diagram of structure formation in the MAA/TEGDMA photopolymerization describing the first four stages is given in Fig. 5.

In the first stage, all reactants are mixed together and UV radiation initiates initiator decomposition to form radicals (shown as filled dots). In the MAA/TEGDMA system with a good solvent, such as the one with a high-ethanol content (ethanol is a good solvent for both hydrophilic MAA and hydrophobic TEGDMA and Irgacure 651 due to its participation in the interactions of hydrogen bonding and esterification), a homogeneous solution is formed with uniform distribution of all reactants. While in a poor solvent with a high water content, TEGDMA tends to form a micelle-like structure due to the amphiphilic properties. Its hydrophilic ends prefer to be in contact with the water phase by hydrogen bonding while the hydrophobic area is located in the center, where most Irgacure 651 molecules are located. This initial structure is verified by the DLS measurement of MAA/-TEGDMA mixtures without UV radiation shown in Fig. 6. In the MAA/TEGDMA system with the 1:4 solvent ratio, no ‘particles’ were observed in the DLS analysis. On the other hand, in the system with the 9:1 solvent ratio, a peak about 6 nm was observed with or without Irgacure 651, supporting the complex formation by amphiphilic TEGDMA.

After initiation, radicals react with monomers to produce monomeric radicals. Because of the presence of multifunctional monomers, the monomeric radicals have chances to link with these molecules to form the growing macroradicals with pendant double bonds, leading to the cyclization or ring formation through intramolecular reactions. The intramolecular reactions consume vinyl groups, but do not contribute to the increase of molecule weight and macroscopic network formation. This internal crosslinking on the primary polymer chains leads to the formation of ‘microgels’ [22]. Inside the microgels, the Trommsdorff effect may occur because termination is largely hindered due to immobilized polymerical radicals, while the propagation rate is less affected since small MAA monomers are still mobile. This results in a small peak or shoulder in the early stage of the reaction profiles. However, the relative viscosity remains nearly unchanged. The greater extent of intramolecular cyclization means less intermolecular crosslinking. This leads to larger mesh size in formed hydrogels, and the weaker mechanical properties. This mechanism of intramolecular cyclization has been used to explain the network formation influenced by the light intensity [8], the solvent concentration [13], the solvent quality [12,14] and the curing temperature [20].

In the solvent mixture, it is favorable for ethanol to participate in the formation of hydrogen bonds with MAA

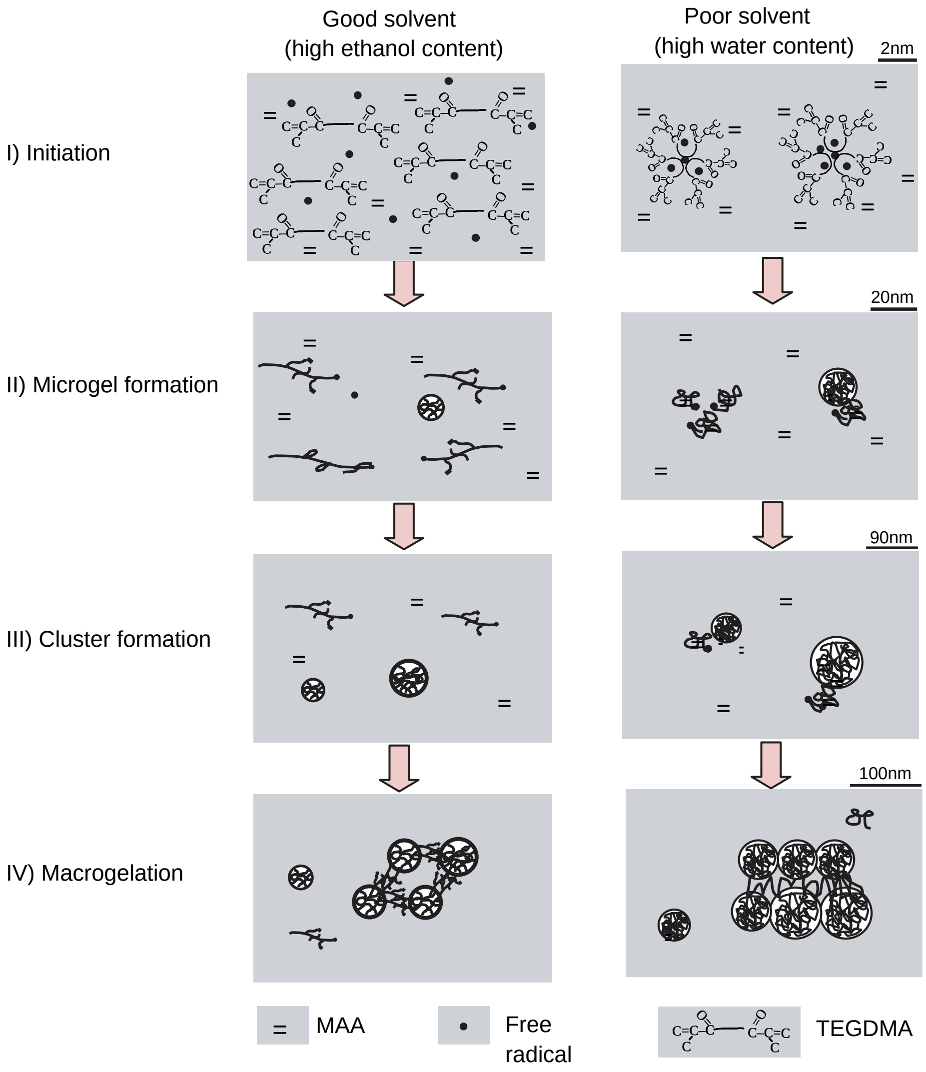

Fig. 5. The schematic diagram of structure formation of MAA/TEGDMA with different solvent qualities.

molecules. Thus, more ethanol means stronger interactions with MAA molecules. Consequently, the overall rate of polymerization would be lower with more ethanol since the propagation can only take place if the propagating macroradical is in the vicinity of the monomer molecules [23]. Furthermore, the uniform distribution of TEGDMA and radicals increases the distance between radicals and free vinyls or pendant vinyls, resulting in a high extent of intramolecular cyclization and the formation of smaller microgels. The solvent composition has little effect on the solution viscosity at this stage since microgel formation does not significantly affect bulk properties in the solution.

During the cluster formation stage (stage III), the reactive microgels with pendant double bonds may react with free monomers and other microgels to form larger clusters, resulting in a bimodal molecular size distribution. The Trommsdorff effect in the clusters leads to the second autoacceleration in the reaction profiles. At the later part of this stage, the presence of a larger number of clusters and

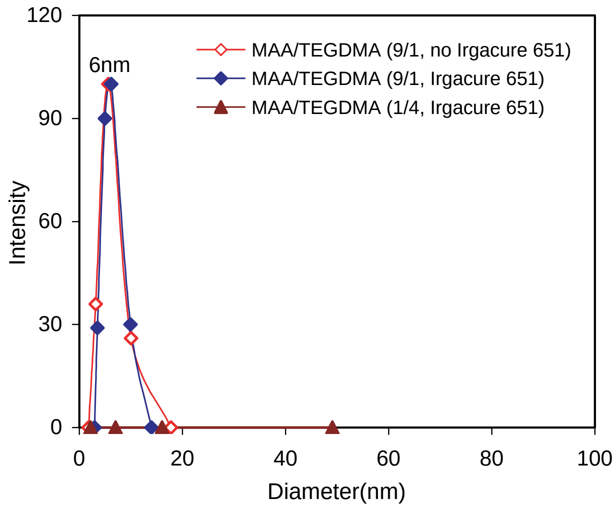

Fig. 6. The size distribution of MAA/TEGDMA monomer solution (1.0% TEGDMA, 50 wt% solvent) with different compositions.

the inter-connection of some clusters lead to an increase of solution viscosity.

As a macroscopic polymeric network is formed by chemical or physical crosslinking, the resin system reaches the gel point in stage IV. Approaching the gel point, most small microgels have converted to the larger clusters and intermolecular reactions among these clusters finally lead to macrogelation. For the transition from microgels to macrogels, intermolecular crosslinking reactions require the displacement of neighboring solvent molecules from the vicinity of the microgels. In the system with a higher water content the microgels can easily form larger aggregates at a higher reaction rate due to the weaker interactions between the microgels and solvent mixture. Therefore, the MAA/TEGDMA with the 9:1 solvent ratio exhibited the shortest gel time and the highest gel conversion as shown in Fig. 3(B). While the uniformly distributed smaller microgels in a system with a higher ethanol content have less chance to connect with each other, taking longer time to reach the gel point. As the system entered the post-gelation stage (V), the reaction rate abruptly decreased since both propagation and termination became diffusion limited.

3.4. Swelling ratio and structural characterization

Fig. 7 compares the equilibrium swelling ratio (SR) in different pH buffer solutions for hydrogels synthesized with various solvent compositions. In all cases, the hydrogel samples swelled more at higher pH due to the electrostatic repulsion between the ionized forms of the carboxylic segments, as well as the dissociation of hydrogen bonds between the carboxylic acid groups of MAA and the oxygen of the ether groups of TEGDMA. In addition, the hydrophilicity of ionized molecules also favors the swelling. Below a pH of 6.0, the swelling ratio drastically decreased, indicating the hydrogel was in a relatively collapsed state mainly due to the formation of hydrogen bonding. It is also interesting to note that the gels with the highest ethanol content had the highest swelling ratio for a specific pH value and its value reached approximately 33 at a pH of 7.3.

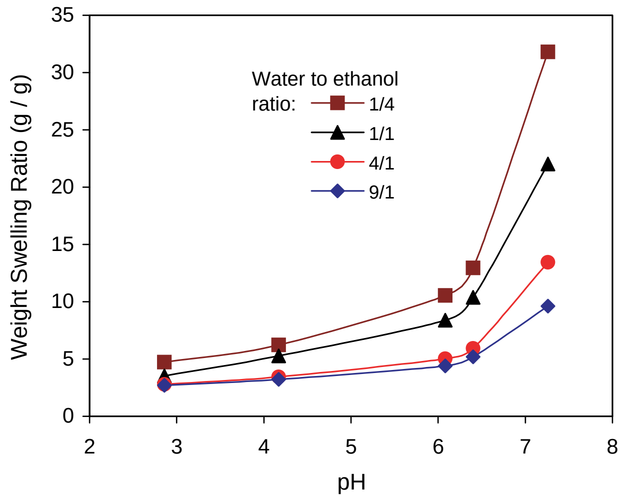

Fig. 7. Equilibrium swelling ratios of the PMAA (1.0 mol% TEGDMA) hydrogels with different solvent ratios as a function of pH values.

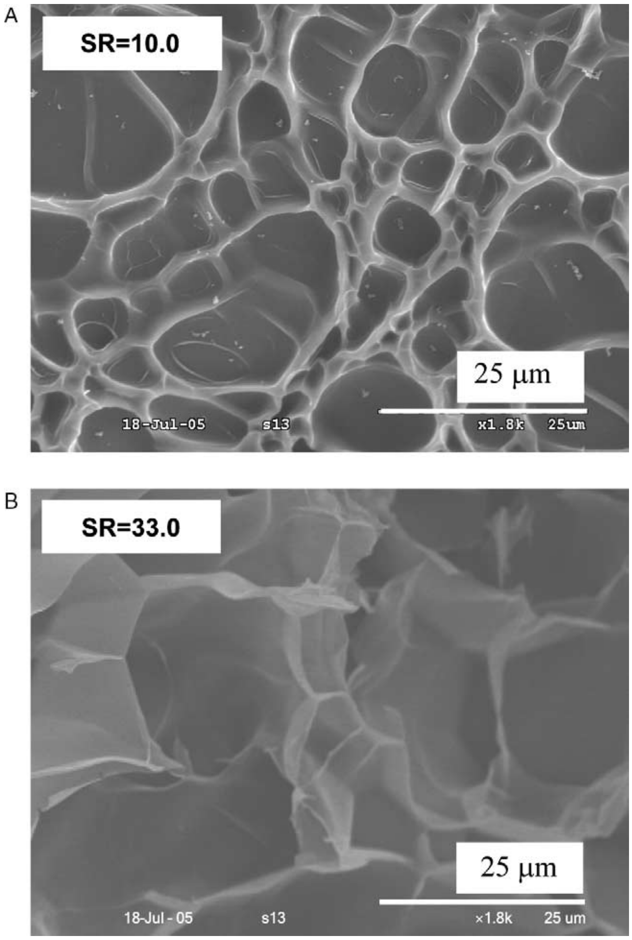

Fig. 8. SEM micrograph of swollen PMAA hydrogels (1.0 mol% TEGDMA, 50 wt% solvent) with different swelling ratios (SR) in pH = 7.4 buffer solution (A) 9:1 and (B) 1:4.

SEM technique is useful to reveal hydrogel structure, although the pre-treatment of dehydration and/or fixation procedures for SEM examination may affect the morphology of a hydrogel [24]. As shown in Fig. 8, the pore structures of the swollen interior of PMAA hydrogels are different depending on the solvent composition. Fig. 8(A) presents the SEM micrograph of PMAA hydrogel with the 9:1 solvent ratio. In a pH = 7.4 buffer solution, this hydrogel (SR = 10.0) exhibited mostly circular and elliptical pores with smaller pores. Its pore size varies from very small to very large pores, which may be a result of inhomogeneous reaction during photopolymerization. On the other hand, the swollen gel with the 1:4 solvent ratio in the same buffer solution showed larger and more uniform pores as shown in Fig. 8(B).

Fig. 9 shows the different morphology of swollen PMAA gels with the same swelling ratio (SR = 4.3) in the freeze–dried state. To obtain the same swelling ratio, the gels with the solvent ratios of 1:4 and 9:1 were immersed in buffer solutions with the pH values of 3.0 and 6.2, respectively. The gel with a higher water content displayed smaller pores and much thicker pore walls at the same SR value.

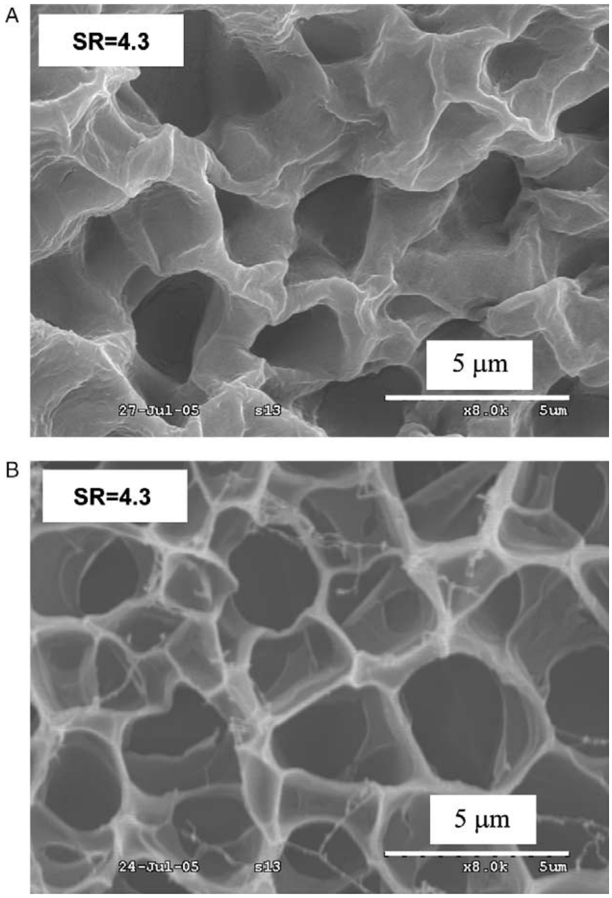

Fig. 9. SEM micrograph of swollen PMAA hydrogels (1.0 mol% TEGDMA, 50 wt% solvent) with the same swelling ratio (SR = 4.3) in different buffer solution: (A) 9:1 in pH = 6.2 buffer (B) 1:4 in pH = 3.0 buffer.

These results are consistent with the solvent effect discussed in the previous section. The localized reactants contribute to the formation of highly crosslinked network structure in the poor solvent, leading to the smaller pores with thicker wall, while the uniformly distributed reactants in a good solvent lead to a looser network structure, forming larger pores with thinner wall.

4. Conclusion

This work clarified the role of the solvent composition in the photopolymerization of hydrogels. The solvent composition has a great influence on the reaction kinetics of photocurable MAA/TEGDMA system. With the increase of the ethanol content in the solvent mixture, the photopolymerization rate and the gel conversion decreased, while the gel time and the swelling ratio of PMAA hydrogels increased.

This can be explained by the solvent compatibility and interaction with the reactants and the initiator. A less ethanol content means weaker interactions between MAA and solvent. This weaker interaction led to a higher reaction rate and a faster gel formation. In addition, the less compatibility resulted in localized TEGDMA and initiator distribution. Since the localized TEGDMA contributed to more highly crosslinked microgels, the resulting hydrogel had a lower swelling ratio and less uniform pore distribution. This mechanism has been confirmed by viscosity measurement, dynamic light scattering analysis, and SEM observation.

Acknowledgements

The authors would like to thank the National Science Foundation funded Center for Advanced Polymer and Composite Engineering (CAPCE) for financial support.

References

[1] Peppas NA, Bures P, Leobandung W. Eur J Pharm Biopharm 2000;50:27–46.
[2] Peppas NA. Curr Opin Colloid Interface Sci 1997;2:531–7.
[3] Lu S, Anseth KS. J Controlled Release 1999;57:291–300.
[4] Ward JH, Peppas NA. J Controlled Release 2001;71:183–92.
[5] Hassan CM, Peppas NA. J Am Chem Soc 1999;54–69.
[6] Crump S. Composites 2001 Convention and Trade Show; 2001, October 3–6.
[7] Jakubiak J. J Polym Sci, Part A: Polym Chem 2000;38(5):876–86.
[8] Li L, Lee LJ. Polymer. 2005; 46(25):11540–7.
[9] Lowman AM, Peppas NA. Macromolecules 1997;30:4959–65.
[10] Anseth KS, Bowman CN, Brannon-Peppas L. Biomaterials 1996;17:1647–57.
[11] Peppas NA. J Bioact Compat Polym 1991;6:241–6.
[12] Kwok AY, Qiao GG, Solomon DH. Polymer 2003;44:6195–203.
[13] Elliott JE, Anseth JW, Bowman CN. Chem Eng Sci 2001;56:3173–84.
[14] Elliott JE, Bowman CN. J Phys Chem B 2002;106(11):2843–7.
[15] Lai YC, Quinn ET. ACS Symp Ser 1997;35–50.
[16] Horie K, Otagawa A, Muraoka M, Mita I. J Polym Sci, Part A: Polym Chem 1975;13(2):445–54.
[17] Cook WD. J Polym Sci, Part A: Polym Chem 1993;31(4):1053–67.
[18] Anseth KS, Wang CM, Bowman CN. Polymer 1994;35(15):3243–50.
[19] Hsu CP, Lee LJ. Polymer 1993;34(21):4516–23.
[20] Chiu YY, Lee LJ. J Polym Sci, Part A: Polym Chem 1995;33:257–67.
[21] Sun XD, Chiu YY, Lee LJ. Ind Eng Chem Res 1997;36:1343–51.
[22] Dusek K, Spevacek J. Polymer 1980;21(7):750–6.
[23] Henrici-Olive G, Olive S. Z Phys Chem (Muenchen, Germany) 1965;47:286–98.
[24] Hong PD, Chen JH. Polymer 1998;32:5809–17.